frontiers | Frontiers in Forests and Global Change

ORIGINAL RESEARCH
published: 25 May 2022
doi: 10.3389/ffgc.2022.879382

Climate Change Increases the Severity and Duration of Soil Water Stress in the Temperate Forest of Eastern North America

Cybèle Cholet[1], *Daniel Houle*[2], *Jean-Daniel Sylvain*[3], *Frédérik Doyon*[1] *and Audrey Maheu*[1]*

[1] *Institut des Sciences de la forêt tempérée, Université du Québec en Outaouais, Ripon, QC, Canada,* [2] *Environnement et Changement Climatique Canada, Montréal, QC, Canada,* [3] *Direction de la Recherche Forestière, Ministère des Forêts, de la Faune et des Parcs, Québec, QC, Canada*

Under climate change, drought conditions are projected to intensify and soil water stress is identified as one of the primary drivers of the decline of forests. While there is strong evidence of such megadisturbance in semi-arid regions, large uncertainties remain in North American temperate forests and fine-scale assessments of future soil water stress are needed to guide adaptation decisions. The objectives of this study were to (i) assess the impact of climate change on the severity and duration of soil water stress in a temperate forest of eastern North America and (ii) identify environmental factors driving the spatial variability of soil water stress levels. We modeled current and future soil moisture at a 1 km resolution with the Canadian Land Surface Scheme (CLASS). Despite a slight increase in precipitation during the growing season, the severity (95*th* percentile of absolute soil water potential) and duration (number of days where absolute soil water potential is greater than or equal to 9,000 hPa) of soil water stress were projected to increase on average by 1,680 hPa and 6.7 days in 80 years under RCP8.5, which correspond to a 33 and 158% increase compared to current levels. The largest increase in severity was projected to occur in areas currently experiencing short periods of soil water stress, while the largest increase in duration is rather likely to occur in areas already experiencing prolonged periods of soil water stress. Soil depth and, to a lesser extent, soil texture, were identified as the main controls of the spatial variability of projected changes in the severity and duration of soil water stress. Overall, these results highlight the need to disentangle impacts associated with an increase in the severity vs. in the duration of soil water stress to guide the management of temperate forests under climate change.

Keywords: soil water stress, Northeast American temperate forests, land surface modeling, climate change, water availability, soil moisture modeling, drought

OPEN ACCESS

Edited by:
Daniel Limehouse McLaughlin, Virginia Tech, United States

Reviewed by:
Leo Separovic, Environment and Climate Change Canada, Canada
Andrew Christopher Oishi, Southern Research Station, Forest Service (USDA), United States

***Correspondence:**
Audrey Maheu
audrey.maheu@uqo.ca

Specialty section:
This article was submitted to Forest Hydrology, a section of the journal Frontiers in Forests and Global Change

Received: *19 February 2022*
Accepted: *21 April 2022*
Published: *25 May 2022*

Citation:
Cholet C, Houle D, Sylvain J-D, Doyon F and Maheu A (2022) Climate Change Increases the Severity and Duration of Soil Water Stress in the Temperate Forest of Eastern North America. Front. For. Glob. Change 5:879382. doi: 10.3389/ffgc.2022.879382

1. INTRODUCTION

Drought conditions are expected to intensify with climate change and projections point toward an increase in the severity, duration and extent of these events (Stocker, 2014; Trenberth et al., 2014; Cook et al., 2015; Samaniego et al., 2018). Widespread drying of the land surface is projected, which can be traced back to an increase in the evaporative demand with warmer air temperatures

(Zhao and Dai, 2015). There is strong evidence for the increase of megadisturbance intensifying drought conditions in regional hot spots (Millar and Stephenson, 2015) characterized by a semi-arid climate such as southwestern North America (Williams et al., 2020), the Mediterranean region (Gudmundsson and Seneviratne, 2016), and southeastern Australia (Cai et al., 2012). In temperate regions, higher uncertainty remains regarding the trajectory of drought conditions but reduced soil moisture is projected over large portions of North America (Cook et al., 2018), with eastern Canadian forests facing a 20–40% reduction in soil moisture by the 2080s (Houle et al., 2012).

These projections suggest a bleak future for forests as water stress has been identified as one of the primary drivers of the global decline of these ecosystems (Allen et al., 2015). In North America, the observed increase in tree mortality has been linked to increasing levels of water stress (Hember et al., 2017; Chaste et al., 2019). Large-scale tree mortality has been documented following drought events in arid regions (Breshears et al., 2005). Forests in humid climates have also not been spared, with water stress leading to reduced growth and increased mortality in these regions (Brzostek et al., 2014; D'Orangeville et al., 2018). As such, the large carbon sinks provided by temperate forests over the past decades (Pan et al., 2011) may be compromised in the future by mild but chronic water stress (Brzostek et al., 2014).

Temperate forests face many challenges that may impact forest net primary productivity (Millar and Stephenson, 2015) and better understanding of water availability is needed to guide future management actions. Various adaptative measures can be implemented to face increasing levels of soil water stress. For example, the reduction of tree density through sylvicultural thinning can increase soil water availability for the remaining trees and has been largely promoted to mitigate soil water stress (D'Amato et al., 2013). However, a better understanding of exposure to soil water stress is still needed to identify priority areas where these measures should be implemented. While large efforts have helped better understand the sensitivity of tree species to drought (Anderegg et al., 2016; Aubin et al., 2016), information on exposure is rarely available at a resolution sufficiently fine for sylvicultural prescription and treatments. For example, global climate models only provide soil moisture projections at a coarse scale (horizontal resolution of ∼300 km). Soil moisture proxies such as the Palmer Drought Severity Index (PDSI) or the Standardized Precipitation Evapotranspiration Index (SPEI) are often used to perform fine-scale assessments of future water stress (Cook et al., 2015). These empirical indices typically assess soil water availability by comparing moisture supply (precipitation) to demand (potential evapotranspiration). Although suitable proxies for past soil moisture trends (Dai et al., 2004; D'Orangeville et al., 2016), these empirical indices have been questioned in climate change assessments given their overestimation of future evaporative demand (Trenberth et al., 2014; Berg and Sheffield, 2018). Moreover, climate data are the sole input of these empirical indices thus ignoring the influence of site conditions (topography, surface deposit thickness, soil texture) and its standing vegetation (composition and structure) on soil moisture.

An adequate understanding of the spatial variability of soil water stress is primordial to improve the prediction of drought-induced tree mortality (Schwantes et al., 2018). Indeed, hydrologic refugia can play a determinant role in buffering water stress (McLaughlin et al., 2017; Costa et al., 2022) while areas exposed to high levels of soil water stress require adaptation measures the most (Grant et al., 2013). Fine-scale assessments of future soil moisture that consider site conditions and standing vegetation are thus crucial to better understand the spatial variability of soil water stress and guide forest management (sylvicultural prescription and treatments) under climate change (Field et al., 2020). This study aims to better understand the trajectory of water stress levels at the northern edge of the North American temperate forest. The objectives of this study were to (i) assess the impact of climate change on the duration and severity of soil water stress and (ii) identify environmental factors driving the spatial variability at the landscape scale of current soil water stress levels and their projected changes.

2. MATERIALS AND METHODS

2.1. Study Area

The study region is located in eastern North America and encompasses the temperate-boreal forest ecotone. It corresponds to the extent of the Outaouais administrative region (34,012 km^2, between latitude 45.37 and 47.85° N and longitude 74.70 and 77.93° W) in the southwestern portion of the province of Quebec, Canada. This region represents one of the driest portions of the Northeast American temperate forest, with average annual precipitation (1981–2010) varying between 847 and 1,088 mm, thus making it a region of particular interest to study soil water stress. The climate is classified as Dfb according to Köppen-Geiger classification, characterizing a fully humid continental climate with warm summer and coldest months averaging below 0°C. Average annual temperatures (1981–2010) in this region vary between 6.3°C in the south to 1.7°C in the north, while average annual total precipitation varies from 900 mm in the west to 1,100 mm in the east (McKenney et al., 2011).

The southern portion is largely dominated by shaded tolerant hardwood tree species (*Acer saccharum*, *Betula alleghaniensis*, *Tilia americana*, *Fagus grandifolia*), unshaded tolerant (*Betula alleghaniensis*, *Betula papyrifera*, *Populus* sp.), and with some conifers (*Tsuga canadensis*, *Abies balsamea*, *Pinus strobus*, and *Picea glauca*). Conifer and unshaded tolerant tree species gain in importance as we move north. Dominant forest types are sugar maple-hickory (6% of the region area), sugar maple-basswood (16%), and sugar maple-yellow birch (42%) in the south, whereas the northern portion is dominated by balsam fir-yellow birch (34%) and balsam fir-white birch (2%) (MFFP, 2018). Soils are mostly podzolic soils, common in cool and humid climate (Sanborn et al., 2011). Soils are generally shallow, often <1 m thick, particularly the ones on the Canadian Shield. Most of these have developed on glacial till deposits and exhibit a large dominance of sandy loam and loamy sand soils throughout the study area.

2.2. Model Description

To assess levels of soil water stress, we performed offline simulations of soil moisture across the study area with the Canadian Land Surface Scheme (CLASS; version 3.6; Verseghy, 2000) within the hydrologic land surface modeling platform MEC—Surface and Hydrology (MESH; version r1552 Pietroniro et al., 2007) developed by Environment and Climate Change Canada (ECCC). CLASS is a physically based land surface model (Verseghy, 2000) that simulates heat and moisture exchanges between the surface and the atmosphere. Forcing data consist of seven input variables at a 30-min time step: downwelling shortwave radiation, downwelling longwave radiation, surface air pressure, air temperature, specific humidity, wind speed, and total precipitation.

For each grid cell, CLASS computes the energy and water budgets separately for four sub-compartments (canopy over snow, canopy over bare ground, bare ground, and snow) and then averages it. Vegetation is described according to four plant functional types (PFT)—needleleaf trees, broadleaf trees, crops, and grass—for which the fractional coverage of each grid cell is defined. Physiological and structural characteristics are assigned representative values for each PFT and these remain constant over the year except for the leaf area index (LAI), which varies seasonally between set minimum and maximum values (Verseghy et al., 1993).

In CLASS, several soil layers can be defined with specific thickness, texture and organic matter content. Vertical movement in the soil layers is governed by a finite difference solution of Richards equation for unsaturated flow in porous media, which balance gravity and capillary forces (Verseghy, 1991). No horizontal flow is allowed and excess water above the soil column is removed depending of the defined allowable depth of ponding. Soulis et al. (2000) noted issues with this approach, leading to the first soil layer remaining too wet between rainfall events. In the present study, we thus used the CLASS model within the MESH platform which allows the activation of the WATROF module that takes into account topography and horizontal flow and computes overland flow and interflow based on approximations of Richards' equation (Soulis et al., 2000; Pietroniro et al., 2007; Mekonnen et al., 2012). Thus, water fluxes were modeled independently as a 1D cell with horizontal flow removed water from grid cells according to the WATROF module. Horizontal flow was then getting out of the system as runoff into surface water and no routing (i.e., transfer between grid cells) was performed.

2.3. Model Implementation

The model was set up with a grid cell resolution of 1 × 1 km representing a total of 34,854 grid cells for the study region. However, for the modeling, we retained only grid cells covered by at least 75% of forest (n = 24,473), as described by the forest cover type (Deciduous, Mixed, Coniferous) from the fifth provincial forest inventory (MFFP, 2018). Because of such filtered selection, we solely used the broadleaf trees and evergreen trees PFT to characterize land cover and computed the proportion of these two PFT in each grid cell based on the weighted average of the forest cover type from the fifth provincial forest inventory. For the mixed forest cover type, we assign 0.5 of the area to each of the two PFT. Structural and physiological characteristics of each PFT were set based on values provided in the CLASS documentation (Verseghy, 2012), except for the maximum LAI and roughness length (**Supplementary Table 1**). The roughness length was calculated from the stand height from the fifth provincial forest inventory (MFFP, 2018). The maximum LAI of each PFT was characterized using the 8-day composite MODIS-LAI data with a 500 m resolution for years 2002–2018 (Myneni et al., 2015). We extracted the annual maximum LAI for each grid cell and then computed the average annual maximum LAI. Given CLASS was little sensitive to the LAI over the study area (Maheu et al., 2021), we set the annual maximum LAI at the PFT level (as opposed to the grid cell level) which we calculated as the median value of all grid cells occupied by more than 75% of the corresponding PFT.

We set the number of soil layers and their corresponding thickness uniformly across the study area, with a progressive increase of the thickness of the layers with depth in order to avoid numerical instability. Nine soil layers were defined for each grid cell with the following depth (m): 0–0.10, 0.10–0.25, 0.25–0.45, 0.45–0.7, 0.7–1.0, 1.0–1.5, 1.5–2.0, 2.0–3.0, and 3.0–5.0 below the surface. The first soil layer was defined as an organic layer in order to represent the superficial layer of humus. Houle et al. (2014) showed that adding a surface organic layer improved the simulation of soil temperature in the deeper soil layers during the summer. This layer could not be set thinner than 0.10 m because of numerical instability. For mineral horizon, we extracted soil properties from the SIIGSOL database (Sylvain et al., 2021) at a 1 km resolution. SIIGSOL database allows to describe the proportion of sand, clay, silt, and organic carbon content along the soil profile. Organic carbon content is converted into organic matter using the Van Bemmelen factor of 1.724. According to the SIIGSOL database, the study area is mainly characterized by sandy loam and loamy sand soils representing 96.2 and 3.7% of the modeled grid cells, respectively. The total soil depth was defined based on superficial deposits of the fifth provincial forest inventory (MFFP, 2018) in which superficial deposits are categorized according to depths according to the following categories: 0–0.5, 0.5–1.0, and > 1 m. Correspondingly, soil depth in CLASS was classified into three categories(0.5, 1, and 2 m), representing 6, 18, and 76% of the modeled grid cells respectively. We defined the slope of each grid cell based on a slope map at a 2 m resolution derived from LiDAR data (MFFP, 2015). The slope value assigned to each grid cell was obtained by first performing a bilinear resampling from a 2 m resolution to a 50 m resolution and then aggregating by average to the 1 km resolution. Last, we defined drainage density for each cell as the total length of all streams and rivers from the Quebec provincial environment ministry (MELCC, 2018) in a cell divided by the total area of the cell.

The performance of the model had been assessed by comparing soil moisture simulations (with the same model implementation) with field measurements at the Duchesnay Forest (Maheu et al., 2021). Results show a good performance of the model during the growing season (between May and October) and demonstrate the ability of CLASS to simulate periods of low

soil moisture and thus its efficiency to characterize soil water stress levels in the study region.

2.4. Climate Data

Using CLASS, we simulated soil moisture for current and future climate conditions. To describe current climate conditions (1981–2010), we used the ERA5 reanalysis dataset (Hersbach et al., 2020), which is the fifth generation atmospheric reanalysis of the global climate released by the European Center for Medium-Range Weather Forecasts (ECMWF). The dataset is produced at a 1-hourly time step on regular latitude-longitude grid at 0.25° resolution. Tarek et al. (2020) showed similar hydrological modeling performance when using the ERA5 reanalysis data and meteorological observations as forcing data in North America. As such, the ERA5 dataset appeared like a good alternative to meteorological observations given the sparse network of weather stations over the study area.

To describe future climate conditions and assess projected changes in water stress levels, we used eight simulations performed by the fifth-generation Canadian Regional Climate Model (CRCM5 Martynov et al., 2013; Šeparović et al., 2013). The regional climate model (RCM) was driven by four global climate models (GCMs) from the fifth Coupled Model Intercomparison Project (CMIP5) ensemble (CRCM5-CANESM2, CRMC5-CNRM-CM5, CRCM5-GFDL-ESM2M, and CRCM5-MPI-ESM-LR) for two different representative concentration pathways (RCP4.5 and RCP8.5). The RCM dataset covers the 1951–2100 period and is produced at a 3-hourly time step (except for precipitation at a 1-hourly time step) on a curvilinear grid at approximately 0.22° resolution. We regridded the dataset to the ERA5 reanalysis grid using bilinear interpolation.

Using CLASS, we simulated soil moisture for each forested grid cell for current (ERA5 reanalysis and historical CRCM5 simulations) and future (CRCM5 simulations) climate conditions. Each variable of forcing data was interpolated at a 30-min time step, as required by CLASS. We used a spin-up period of 30 years (1951–1980 period) to ensure stable initial condition of soil water content. Simulations under future climate conditions were performed with fixed vegetation conditions, which correspond to current conditions (see Section 2.3). We described current climate conditions (1981–2010) during the growing season (May–October, MJJASO) as well as changes in climate conditions between future (2050s and 2080s, characterizing 2041–2070 and 2071–2100 periods, respectively) and reference periods (1981–2010) from historical CRCM5 simulations, using five climate indices: PSUM is the total precipitation (mm), P1 is the number of dry days (precipitation $\leq$ 1 mm) (days), TX is the mean of daily maximum temperature (°C), WSDX is the maximum duration of warm spells defined as the largest number of consecutive days daily max temperature $\geq$ 25°C (days) and VPDX is the mean of daily maximum vapor pressure deficit (kPa).

2.5. Characterizing Soil Water Stress Levels

To assess soil water stress levels, we first converted the volumetric soil water content ($m^3.m^{-3}$) simulated by CLASS into daily maximum absolute soil water potential (hPa) by applying the (Clapp and Hornberger, 1978) water retention curve implemented in CLASS (Verseghy, 2012). Soil water potential, rather than volumetric water content, is more representative of water availability because it takes into account soil properties and reflects the amount of energy that vegetation must provide to extract water from the soil. We computed two indices based on soil water potential to characterize the severity (S) and the duration (D) of the water stress. The severity index S was defined as the 95th percentile of the absolute soil water potential (hPa) and the duration index D was defined as the mean number of days per year where absolute soil water potential $\geq$ 9,000 hPa. This threshold was chosen to characterize intermediate water stress conditions and corresponds approximately to the 85th percentile of the S index of all modeled cells under current climate conditions. Both indices, S and D, were computed on the second soil layer defined at a depth of 0.10–0.25 m, where most tree roots are concentrated (Jackson et al., 1996; Tauc et al., 2020). Soil water stress indices were computed for the growing season (MJJASO) over 30-year periods to characterize, on the one hand, the current levels of water stress (forcing data = ERA5 reanalyses) and on the other hand, the mean projected changes (forcing data = CRCM5 simulations associated with RCP4.5 and RCP8.5). We used the anomaly method (Déqué, 2007) to assess projected changes in water stress indices (ΔS and ΔD) calculated for 30-year periods. Accordingly, we assessed changes in water stress levels between a future period (2041–2070 and 2071–2100) and a reference period (1981–2010) of the CRMC5 simulations. We calculated projected changes in water stress levels for each of the eight RCM simulations, which we then averaged for each RCP in order to obtain the average projected changes and associated standard deviation for each modeled grid cell. Results shown in this study mainly focus on RCP8.5, representing a worst-case scenario where air temperatures increase by 4.9°C by the end of the century compared to preindustrial levels.

2.6. Environmental Controls of Water Stress Duration and Severity

Random forest regressions (Breiman, 2001; Cutler et al., 2012) were used to identify environmental factors that are controls of soil water stress levels. Inputs of CLASS were used as predictor variables (soil depth, soil texture, organic content, slope, drainage density). We fitted independent random forest regressions for current water stress levels S and D and each projected changes in water stress levels (ΔS and ΔD for both RCP4.5 and RCP8.5) using the Python package scikit-learn (1.4.1). Each dataset was randomly split into training (67%) and testing (33%) sets. The hyperparameters of random forest regressions (number of trees in the forest, maximum depth, minimum number of samples required to split an internal node and minimum number of samples required to be at a leaf node) were optimized by using an exhaustive search with a 10-fold cross-validation grid-search over a parameter grid. Selected parameters from optimization searches for each random forest can be found in **Supplementary Table 2**. The mean squared error (MSE) was used as the minimization criteria at each split whereas the coefficient of determination (R^2)

TABLE 1 | Climate indices for the MJJASO period over the study region for current (1981–2010) climate conditions as computed from ERA5 reanalysis data and future climate conditions computed from CRCM5 simulations for the 2050s (2041–2070) and the 2080s (2071–2100).

				PSUM	P1	TX	WSDX	VPDX
Current climate	ERA5	1981–2010	Mean	585 mm	107.2 days	18.8°C	14.3 days	1.11 kPa
			std	30.2 mm	4.0 days	1.2 °C	4.9 days	0.11 kPa
Projected changes	RCP 4.5	2041–2070	Δmean	15.8 mm	2.4 days	2.0°C	9.0 days	0.15 kPa
in future climate			Δstd	3.9 mm	0.01 days	0.3°C	8.4 days	0.06 kPa
			r.c.	2.4%	2.3%	N/A	68.8%	14.6%
		2071–2100	ΔMean	34.9 mm	1.7 days	2.6°C	15.5 days	0.20 kPa
			ΔStd	4.2 mm	0.17 days	0.5°C	13.6 days	0.07 kPa
			r.c.	5.4%	1.5%	N/A	118.6%	18.9%
	RCP 8.5	2041–2070	ΔMean	39.4 mm	2.3 days	2.9°C	19.7 days	0.24 kPa
			ΔStd	10.9 mm	0.18 days	0.4°C	18.9 days	0.07 kPa
			r.c.	6.1%	2.2%	N/A	150.2%	22.2%
		2071–2100	ΔMean	73.2 mm	2.7 days	4.9°C	37.8 days	0.41 kPa
			ΔStd	20.2 mm	0.15 days	0.8°C	24.7 days	0.02 kPa
			r.c.	11.4%	2.5%	N/A	288.2%	37.6%

PSUM is the total precipitation (mm), P1 is the number of dry days (precipitation ≤1 mm) (days), TX is the mean of daily maximum temperature (°C), WSDX is the maximum duration of warm spells defined as the largest number of consecutive days daily max temperature ≥25°C (days) and VPDX is the mean of daily maximum vapor pressure deficit (kPa). ΔMean and Δstd correspond to absolute difference of mean and standard-deviation of projected changes respectively, when r.c. corresponds to mean relative changes in percentage.

was used for the selection of hyperparameters and the assessment of the performance of predictions on the testing set. In addition, we computed the root mean square error (RMSE) and the mean absolute error (MAE) of the testing set. To characterize the relative importance of each predictor variable on the soil water stress levels, we computed the normalized total reduction of the mean squared root criterion brought by that variable. For a given predictor variable, a large value of relative importance indicates the substantial role of this variable to predict soil water stress.

3. RESULTS

3.1. Current Climate Conditions and Soil Water Stress Levels

Under current climate conditions, the study region averaged 585 mm of total precipitation for the growing season (**Table 1**). During this period, average air temperature was 18.8°C with the maximum duration of warm spells averaging 14 consecutive days. The mean of daily maximum vapor pressure deficit was 1.11 kPa. Simulations with CLASS showed that the severity of soil water stress S (95th percentile of the absolute soil water potential) was on average 5,680 hPa under current climate conditions, with a maximum value close to 13,500 hPa and 16% of cells showing a S value higher than 9,000 hPa (**Figure 1A**). Maximum S values were found in central and southwestern areas of the study region. The duration of soil water stress D (number of days where absolute soil water potential ≥ 9,000 hPa) was on average 4.5 days, with a maximum value of 35 days and 15% of cells with a D higher than 10 days (**Figure 1B**). Areas where D is >10 days were mainly located in central and southwestern parts of the study region, which also correspond to areas with high values of S.

3.2. Projected Changes in Climate Conditions and Soil Water Stress Levels

Mean projected changes of climate indices for the growing season in the study region are summarized in **Table 1**. Mean total precipitation was projected to increase for both RCP, with an average increase of 6% in the 2050s and 11% in the 2080s for RCP8.5. The number of precipitation events was projected to remain relatively stable, with a 2.5% increase in the number of dry days in the 2080s for RCP8.5. These changes would thus translate into a number of precipitation events similar to actual conditions, but of greater intensity. A strong warming trend is projected for the growing season, with a 2.9 and 4.9°C increase in maximum daily temperature in the 2050s and 2080s for RCP8.5. This translates into almost a threefold increase in the maximum duration of warm spells and a 38% increase in the maximum daily vapor pressure deficit in the 2080s. The largest projected increases of the evaporative demand, as described by the VPDX, are located in the southwestern part of the study area (**Supplementary Figure 3**).

Overall, simulations with CLASS showed that projected changes in climate lead to an increase in the severity and duration of soil water stress levels over the study region, although with considerable spatial variability in the magnitude of changes (**Figures 1C–F**). Projected changes in the severity of soil water stress (ΔS) indicated a 25 and 33% increase compared to current conditions in the 2080s for RCP4.5 and RCP8.5, respectively. Large ΔS were projected to occur in the central and northern parts of the study region, with maximum increases of ∼3,220 and 3,470 hPa for RCP4.5 and RCP8.5, respectively. Projected changes in the duration of soil water stress ΔD indicated an average increase of 108% for RCP4.5 and 158% for RCP8.5 in the 2080s. The largest projected increases of ΔD, 12 days for RCP4.5

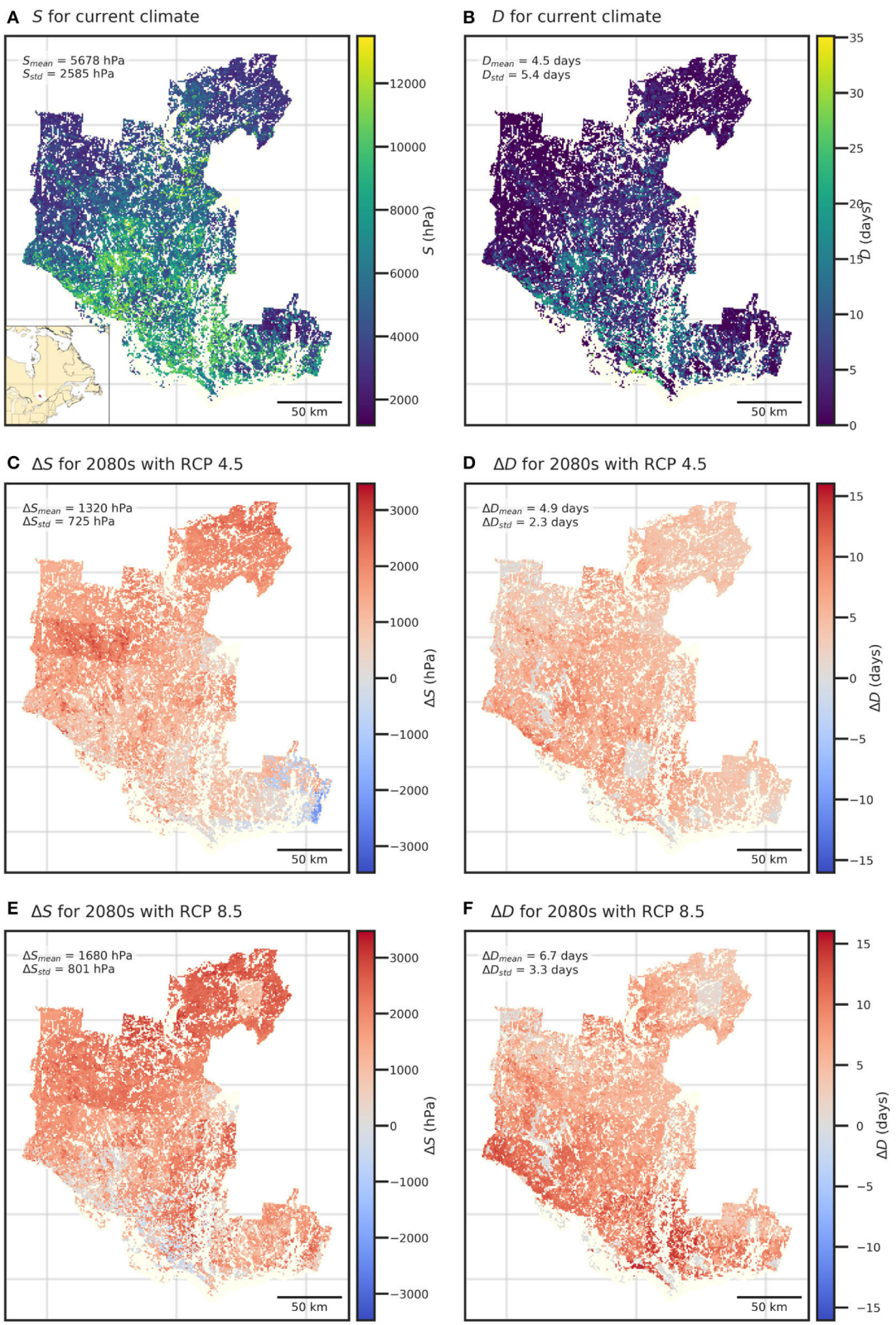

FIGURE 1 | Spatial distribution of the severity S and duration D of soil water stress under current climate conditions **(A,B)** and projected changes ΔS and ΔD for RCP4.5 **(C,D)** and RCP8.5 **(E,F)** for the 2080s. Ivory colored cells correspond to non-forested areas, i.e., grid cells with <75% of forest cover.

and 16 days for RCP8.5, were located in the southwestern part of the study region.

The largest projected changes in ΔS and ΔD occurred in different areas of the study region (**Figures 1C–F**). **Figure 2A** illustrates the frequency distribution of D for the current climate. Accordingly, the current duration of soil water stress was less than 3.5 days for 58% of modeled cells, varied between 3.5 and 10.5 days for 29% of cells, varied between 10 and 21 days for 12% of modeled cells and finally, for only 1% of cells exceeded 21.5 days. For each of the 20 categories (bins) shown for the histogram of D (**Figure 2A**), the respective mean and standard deviation of ΔD (**Figure 2B**) and ΔS (**Figure 2C**) were computed for the 2080s period for both RCPs. Grid cells with current prolonged periods of soil water stress (large D values) showed the largest projected increases in the duration of water stress ΔD while there was no to little projected changes in severity (S) for these cells. For example, grid cells with the lowest values of D (D ≤ 1 day) had a projected increase ΔD of 3–4 days while cells with the largest values of D (D > 10.5 days) had a projected increase ΔD of 6–15 days. At the opposite, the largest projected increase in severity (ΔS = 1,600 hPa for RCP4.5 and 2,000 hPa for RCP8.5) occurred for cells where current soil water stress was of short duration (D ≤ 1 day).

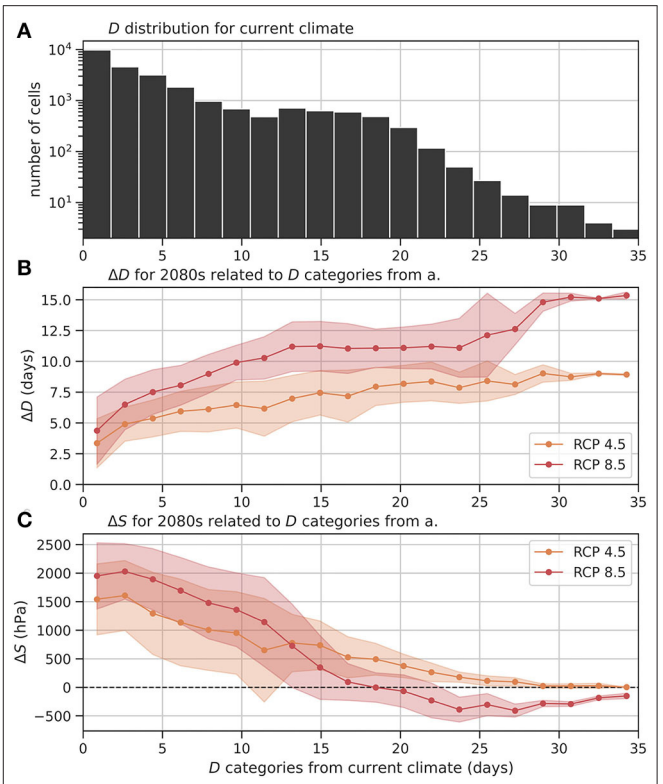

FIGURE 2 | Frequency distribution of duration D of soil water stress for the current climate (1981–2010) for the growing season (MJJASO) **(A)**, associated projected changes in the duration ΔD **(B)**, and in the severity ΔS **(C)** in 2080s (2071–2100) calculated for RCP4.5 and RCP8.5 for categories (bins) defined in **(A)**. In **(B,C)**, points represent the mean of the projected changes for each category of the histogram **(A)** and the band represents the mean value plus and minus one standard deviation.

3.3. Environmental Controls of Current and Projected Changes in Soil Water Stress Levels

Random forest regressions performed on S, D, ΔS, and ΔD showed satisfactory performance with R^2 values >0.72 for current climate conditions and between 0.40 and 0.68 for projected changes (**Figure 3**) after random forest parameters were optimized. As shown by the relative importance of predictor variables (i.e., normalized total reduction of the mean squared root criterion brought by that variable), soil depth was a determinant factor controlling the severity and duration of soil water stress in the current climate (relative importance = 66% for S and 61% for D). Soil depth also played a key role in the projected changes in the severity and duration of soil water stress levels (relative importance = 32–51% for ΔS and 27–35% for ΔD under RCP4.5 and RCP8.5), although to a lesser extent than under the current climate conditions. Soil texture played an increasingly important role with projected changes in climate. For example, the relative importance of clay proportion to explain soil water stress reached 15% for ΔS and 19% for ΔD under RCP8.5.

Under current climate conditions, shallow soils (soil depth = 0.5 m) had the largest levels of soil water stress both in terms of severity (average S = 9,810 hPa, **Figure 4A**) and duration (average D = 13.1 days, **Figure 4C**). In deep soils (soil depth = 2 m), water stress levels were much smaller in terms of severity (average S = 4,140 hPa) and duration (average D = 1.6 days). Projected changes in S were greater in deep soils than in shallow soils, with the largest increase in ΔS for soil depths of 1 m (average ΔS = 1,780 hPa) and 2 m (average ΔS = 2,050 hPa, **Figure 4B**). Important increases in ΔD was projected for all soil depths, with the greatest changes in shallow soils (soil depth = 0.5 m) with an average ΔD of 9.9 vs. 5.2 days for deep soils (soil depth = 2 m, **Figure 4D**). Although current exposure to water stress is greater in shallow soils in terms of severity and duration, projected changes indicate that all soil depths are to see an increase in soil water stress by the 2080s. Overall, shallow soils (0.5 m) are projected to mainly experience an increase in the duration of water stress while deeper soils (1 and 2 m) are projected to mainly see an increase in the severity of water stress. In addition to soil depth, soil texture was also an important control of soil water stress under climate change (**Figure 3**). Under the current climate, areas with the largest S corresponded to soils with a high percentage of sand and low percentages of clay and silt and these were the same areas that experienced the largest ΔS (**Supplementary Figures 1**, **2**).

4. DISCUSSION

4.1. Temperate Forests Currently Experience Soil Water Stress

As shown by simulations under the current climate (**Figure 1**), mild soil water stress presently occurs over the study region, with mean S close to 5,600 hPa. The study region experiences only a few days of intermediate water stress, with about 5 days

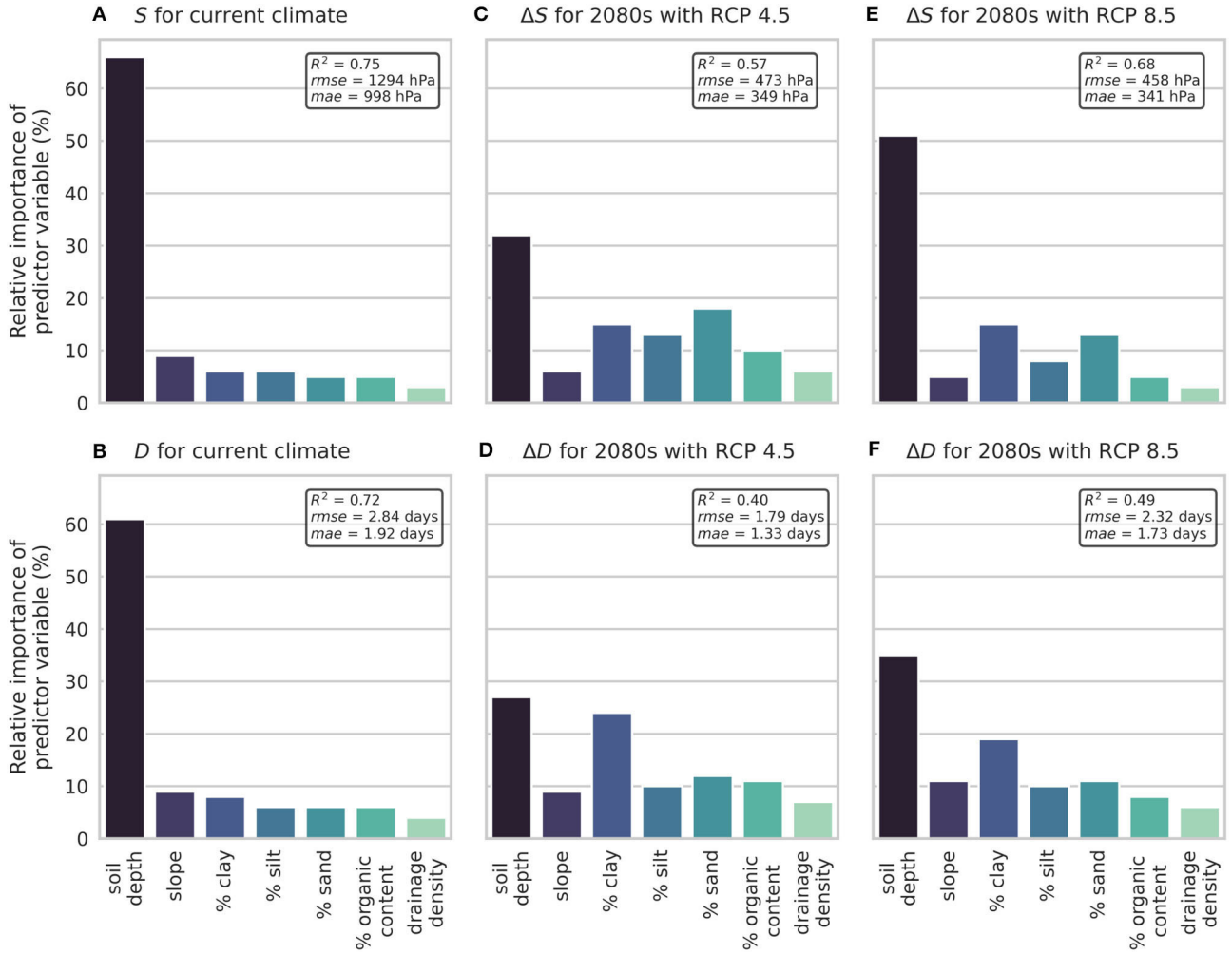

FIGURE 3 | Relative importance of predictor variables for **(A,B)** the severity S and duration D of soil water stress levels for the growing season (MJJASO) under current (1981–2010) climate conditions as well as for the projected changes in **(C,D)** the severity (ΔS) and **(E,F)** the duration (ΔD) of soil water stress levels under future climate conditions for the 2080s (2071–2100). Also shown is the root mean square error (RMSE) and the mean average error (MAE) of the random forest regressions.

per year with absolute soil water potential above 9,000 hPa. These values of soil water potential are typically associated with the onset of soil water stress in temperate forests. For example, in mid-latitude temperate forests dominated by red maple, stomatal resistance began when absolute soil water potential reached 6,000–9,000 hPa (Pettijohn et al., 2009). In European temperate forests, median critical thresholds of absolute soil water potential of plant water stress were estimated to 6,000 hPa with large variability (from 1,000 to 11,000 hPa) between sites (Fu et al., 2021). While mild soil water stress is pervasive across the study region, considerable spatial variability exists and severe water stress currently occurs over the study area, with S approaching the wilting point (15,000 hPa) and exceeding 12,000 hPa in certain locations (**Figure 1**). Certain areas also currently experience prolonged periods of soil water stress during the growing season, with absolute soil water potential above 9,000 hPa for more than 30 days (**Figure 2A**). Both the mild and severe water stress levels found in this study can affect the functioning of temperate forests. On the one hand, mild but chronic water stress can affect the phenology of wood production and thus reduce the carbon sink in deciduous forests (Brzostek et al., 2014), while also reducing soil carbon sequestration (Schindlbacher et al., 2012). On the other hand, severe water stress can lead to widespread dieback (Hoffmann et al., 2011) and eventually the conversion of forests to new ecosystems with the associated loss of ecosystem services (Millar and Stephenson, 2015).

Setting soil water stress thresholds to guide the interpretation of modeling studies such as this one can be challenging. Temperate deciduous tree species denote large differences in water use (Sperry et al., 2002), physiological responses to drought (Ranney et al., 1990), and resilience to drought (Gazol et al., 2018). While thresholds indicative of water stress are typically identified for a given species (Ruffault et al., 2013;

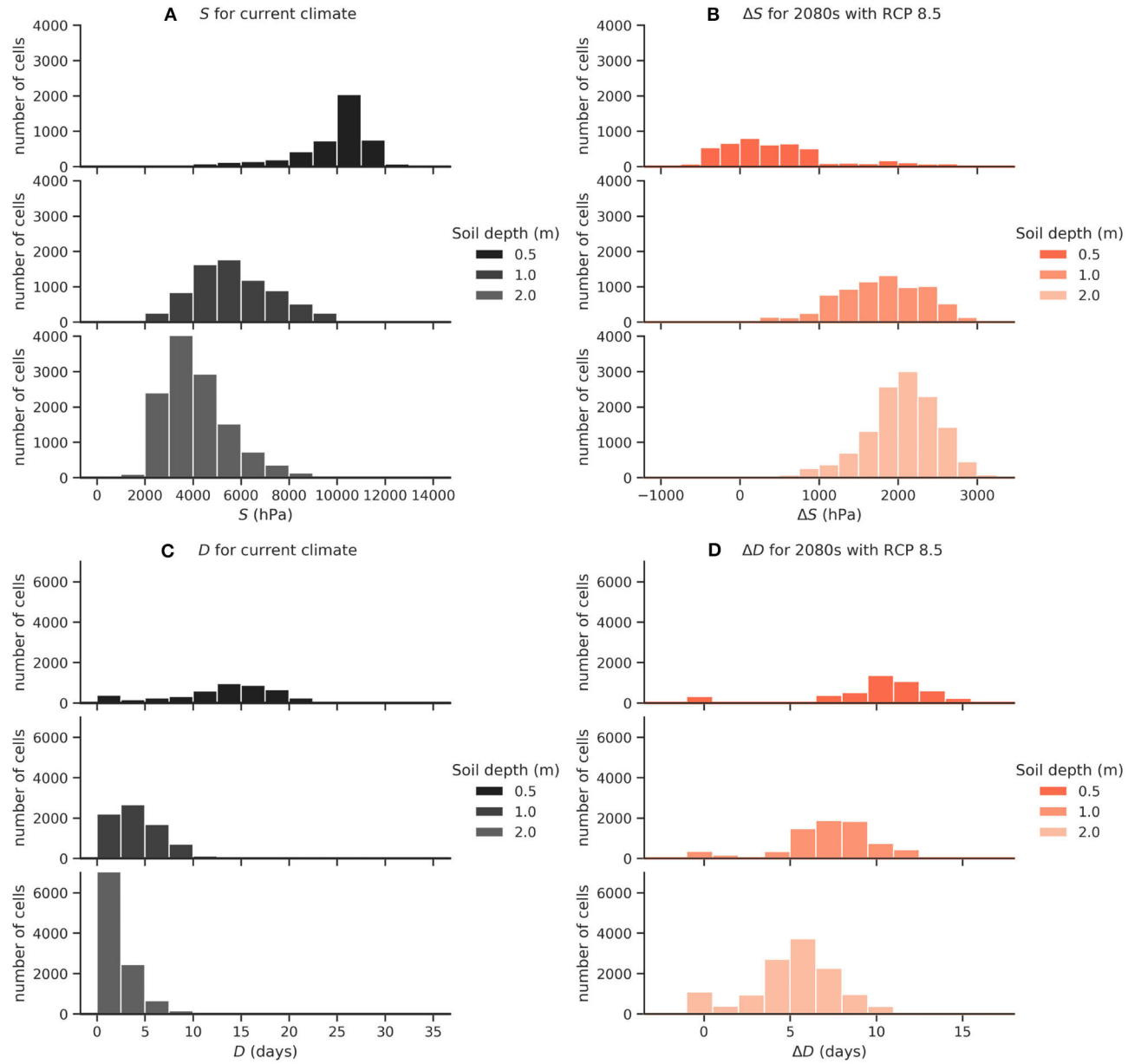

FIGURE 4 | Frequency distribution for the growing season (MJJASO) of **(A)** the severity S for current climate conditions (1981–2010), **(B)** the projected changes in the severity ΔS for 2080s (2071–2100) with RCP8.5, **(C)** the duration D for current climate conditions (1981–2010) and **(D)** the projected changes in the duration ΔD for 2080s (2071–2100) with RCP8.5 computed for the three soil depth categories.

Eckes-Shephard et al., 2021), this study modeled soil moisture at a resolution of 1 km which is not necessary representative of soil water stress levels at the tree scale. Soil moisture can exhibit considerable fine-scale heterogeneity (He et al., 2014) thus leading to a mismatch between modeled values and soil moisture experienced by trees. Overall, a better understanding of soil water stress thresholds at the stand or landscape scales is needed to better assess the response of forests to climate change.

4.2. Projected Increase in Soil Water Stress Severity and Duration, but Not Concomitantly

During the growing season, the largest ΔS at the 2080 horizon are projected to occur at different locations than the largest ΔD (**Figures 1**, **2**). Indeed, the largest ΔS are projected in areas where soil moisture is currently available, i.e., absolute soil water potential rises above 9,000 hPa <5 days per year on average. As such, large increases in severity will affect areas

which until now have been little impacted and are thus probably poorly adapted to soil water stress. At the opposite, the largest ΔD are projected in areas currently experiencing prolonged periods (>25 days) of soil water stress during the growing season. It remains difficult to predict the response of temperate forests to prolonged water limitations (Gerten et al., 2008) as most drought impact studies have focused on extreme and severe events.

The observed pattern, large D values coinciding with large ΔD but small ΔS values, can be explained by the fact that severity can more easily increase in areas experiencing low levels of soil water stress. Indeed, as a soil dries up, more work is required to remove the remaining water molecules tightly bound to soil particles. As such, it becomes increasingly difficult for absolute soil water potential to continue rising thus in turn favoring an increase in the duration of soil water stress. Overall, these results suggest the need to disentangle impacts associated with an increase in the severity vs. in the duration of soil water stress, rarely addressed by experimental studies. Further work is needed to understand in situ response of mature trees to soil water stress with differing combinations of severity and duration, similar to what can be studied using controlled experiments for potted plants (Marchin et al., 2020). Among the limitations of this modeling exercise, some are raising complex issues. First, projected increases in the severity and the duration of soil water stress were computed for the growing season considered as the period between May and October (MJJASO). However, the growing season is projected to lengthen (Christiansen et al., 2011) which could amplify our results given a potential increase in water use by vegetation as a result of a longer growing season. Second, vegetation characteristics remained fixed to current conditions and as such, projected changes in soil moisture do not consider potential changes in vegetation. This assumption appears reasonable in the medium term but could influence projected changes in the severity and duration of soil water stress in the long term.

4.3. Projected Increase in Soil Water Stress Despite Slight Increase in Precipitation

Along with increasing air temperatures, temperate regions are projected to face changes in their precipitation regime, with an increase in total precipitation combined with an increase in the number of dry days (Sushama et al., 2010; Stocker, 2014). In the present study, projected climate change was in agreement with previous studies, with a large increase in maximum daily temperatures and a small increase in total precipitation during the growing season (**Table 1**). Due to the physics of global climate models, various studies have described a positive bias on simulated precipitation (May, 2008; Sushama et al., 2010). Thus, the number of dry days may have been underestimated in the present study, with potential impact on the modeled severity and duration of soil water stress.

Despite an increase in precipitation during the growing season, the present study projected a considerable increase in levels of soil water stress in the future. These results emphasize the importance of modeling the soil water balance to adequately characterize future soil water availability (Hember et al., 2017). Indeed, changes in the atmospheric water demand, as shown by the 38% increase in growing-season VPDX in the 2080s with RCP8.5 (**Table 1**), promote an increase in terrestrial evaporation which can be linked back to increasing levels of soil water stress projected over the study region. Ficklin and Novick (2017) have reported a similar drying atmospheric trend in the United States with a 51% increase in summer VPD between the recent past (1979–2013) and the future (2065–2099). Past increases in the atmospheric water demand have been associated with a reduction in vegetation growth in temperate regions (Babst et al., 2019; Yuan et al., 2019) and modeling studies such as this one can help understand the local response of soil humidity to a future rise in VPD.

4.4. Soil Properties Largely Explain Spatial Variability in Soil Water Stress

Soil depth was the main environmental control of the spatial variability of both current and projected changes in soil water stress (**Figure 3**). Soil texture also becomes an important control of soil water stress under future climate change. Various studies have highlighted the important role of soil properties to explain soil water stress (Schwantes et al., 2018), spatial variability of soil moisture threshold of plant water stress (Fu et al., 2021) and tree mortality (Crouchet et al., 2019). The importance of soil properties toward soil water stress is in part influenced by the choice of the model used to simulate soil moisture and its sensitivity to input variables. As highlighted by Haghnegahdar et al. (2015) in a global sensitivity analysis, soil depth appears as one of the most influential parameters when using CLASS to simulate streamflow. Large uncertainty can be associated with land-surface model structure when simulating the response of hydrological drought to climate change (Prudhomme et al., 2014). Ensemble predictions using several land-surface models may help alleviate this issue, but would require a large computational demand given the fine resolution of the simulations in the present study. Moreover, the importance of soil depth as a control of soil water stress may also stem from the parameterization of soil and root depths in the model as well as the focus given to the soil layer at a 0.10–0.25 m depth when characterizing the severity and duration of soil water stress. When total soil depth is small, roots can only access water from a relatively small volume of superficial soil layers and will mainly extract water in superficial soil layers (i.e., 0.10–0.25 m) thus promoting soil water stress. When total soil depth is large, roots can potentially tap water in deep soil layers thus reducing extraction and the ensuing soil water stress in superficial soil layers. Accordingly, vertical root distribution plays a key role toward soil water in a given layer, as shown by empirical (Yu et al., 2007) and modeling (Stevens et al., 2020) studies. This highlights the need to pursue efforts toward a more realistic representation of root water uptake in land surface models (Vanderborght et al., 2021). Indeed, while climate data are becoming increasingly available at fine spatial resolutions, the challenge lies in reaching a similar level of details when

describing land surface conditions such as soil and vegetation characteristics (Fisher and Koven, 2020). The use of the SIIGSOL database in the present study, which described soil properties at a 250 m resolution, was a step in this direction but further efforts are needed to improve the availability of model inputs quality describing soil and vegetation characteristics and this, at finer scale.

4.5. Implication for the Management of Temperate Forests

Refining the spatial grain for modeling soil moisture offers a promising tool to guide strategies to reduce current and future water stress in forests (Grant et al., 2013). Indeed, locally assessed vulnerability is a crucial requirement for selecting the best approach to promote the adaptation of forests to climate among a portfolio of management options (Royer-Tardif et al., 2021). Using the CLASS land surface model, we simulated soil moisture to identify areas most exposed to soil water stress in temperate forests at the grain size of 1 km^2. When combined with sensitivity information (like in Boisvert-Marsh et al., 2020), the exposure maps this research has generated offer useful tools for ranking vulnerability of the stands to drought and allow the set priorities when planning adaptation strategies in a forest management unit. Forest management practices, such as selective thinning (D'Amato et al., 2013) or facilitating for drought-tolerant species (Grant et al., 2013) can then be implemented at the most appropriate sites. In targeted areas where conservation is critical, novel intensive measures such as irrigation, small-scale impoundments to capture overland flow, soil amendments as well as enhanced root development in nursery-grown tree seedlings can also be implemented (Field et al., 2020). Last, the fine-scale hydrological modeling performed in this study can also help locate and protect hydrologic refugia that support the persistence of local species in the face of climate change (McLaughlin et al., 2017). We highly recommend mainstreaming actual and projected soil moisture information with ecological classification tools in order to facilitate its applicability and rapid use by practitioners (Saucier et al., 2009; Grondin et al., 2018).

DATA AVAILABILITY STATEMENT

The datasets presented in this study can be found in online repositories. The names of the repository/repositories and accession number(s) can be found at: doi: 10.5281/zenodo.6059351.

AUTHOR CONTRIBUTIONS

FD, DH, and AM conceived the idea. J-DS provided the SIIGSOL dataset at the model resolution. CC performed the modeling and analyses. CC and AM drafted the manuscript with contribution of FD, DH, and J-DS. All authors contributed to the article and approved the submitted version.

FUNDING

This research was supported by the Ministère des Forêts, de la Faune et des Parcs (MFFP) du Québec (CRDPJ 536581-18).

ACKNOWLEDGMENTS

We thank Ouranos which provided the CRCM5 dataset. We thank Daniel Princz from the University of Saskatchewan for help with the implementation of CLASS within MESH. Computations were made on the supercomputer Béluga from the École de technologie supérieure de Montréal, managed by Calcul Québec and Compute Canada. The operation of this supercomputer is funded by the Canada Foundation for Innovation (CFI), the Ministère de l'Économie, de la Science et de l'Innovation du Québec (MESI) and the Fonds de recherche du Québec—Nature et technologies (FRQNT). We also thank the two reviewers for their valuable comments on our manuscript.

SUPPLEMENTARY MATERIAL

The Supplementary Material for this article can be found online at: https://www.frontiersin.org/articles/10.3389/ffgc.2022.879382/full#supplementary-material

REFERENCES

Allen, C. D., Breshears, D. D., and McDowell, N. G. (2015). On underestimation of global vulnerability to tree mortality and forest die-off from hotter drought in the anthropocene. *Ecosphere* 6, 1–55. doi: 10.1890/ES15-00203.1

Anderegg, W. R., Klein, T., Bartlett, M., Sack, L., Pellegrini, A. F., Choat, B., et al. (2016). Meta-analysis reveals that hydraulic traits explain cross-species patterns of drought-induced tree mortality across the globe. *Proc. Natl. Acad. Sci. U.S.A.* 113, 5024–5029. doi: 10.1073/pnas.1525678113

Aubin, I., Munson, A., Cardou, F., Burton, P., Isabel, N., Pedlar, J., et al. (2016). Traits to stay, traits to move: a review of functional traits to assess sensitivity and adaptive capacity of temperate and boreal trees to climate change. *Environ. Rev.* 24, 164–186. doi: 10.1139/er-2015-0072

Babst, F., Bouriaud, O., Poulter, B., Trouet, V., Girardin, M. P., and Frank, D. C. (2019). Twentieth century redistribution in climatic drivers of global tree growth. *Sci. Adv.* 5:eaat4313. doi: 10.1126/sciadv.aat4313

Berg, A., and Sheffield, J. (2018). Climate change and drought: the soil moisture perspective. *Curr. Clim. Change Rep.* 4, 180–191. doi: 10.1007/s40641-018-0095-0

Boisvert-Marsh, L., Royer-Tardif, S., Nolet, P., Doyon, F., and Aubin, I. (2020). Using a trait-based approach to compare tree species sensitivity to climate change stressors in eastern Canada and inform adaptation practices. *Forests.* 11, 989. doi: 10.3390/f11090989

Breiman, L. (2001). Random forests. *Mach. Learn.* 45, 5–32. doi: 10.1023/A:1010933404324

Breshears, D. D., Cobb, N. S., Rich, P. M., Price, K. P., Allen, C. D., Balice, R. G., et al. (2005). Regional vegetation die-off in response to global-change-type drought. *Proc. Natl. Acad. Sci. U.S.A.* 102, 15144–15148. doi: 10.1073/pnas.0505734102

Brzostek, E. R., Dragoni, D., Schmid, H. P., Rahman, A. F., Sims, D., Wayson, C. A., et al. (2014). Chronic water stress reduces tree growth and the carbon sink of deciduous hardwood forests. *Glob. Change Biol.* 20, 2531–2539. doi: 10.1111/gcb.12528

Cai, W., Cowan, T., and Thatcher, M. (2012). Rainfall reductions over southern hemisphere semi-arid regions: the role of subtropical dry zone expansion. *Sci. Rep*. 2, 1–5. doi: 10.1038/srep00702

Chaste, E., Girardin, M. P., Kaplan, J. O., Bergeron, Y., and Hély, C. (2019). Increases in heat-induced tree mortality could drive reductions of biomass resources in Canada's managed boreal forest. *Landsc. Ecol*. 34, 403–426. doi: 10.1007/s10980-019-00780-4

Christiansen, D. E., Markstrom, S. L., and Hay, L. E. (2011). Impacts of climate change on the growing season in the United States. *Earth Interact*. 15, 1–17. doi: 10.1175/2011EI376.1

Clapp, R. B., and Hornberger, G. M. (1978). Empirical equations for some soil hydraulic properties. *Water Resour. Res*. 14, 601–604. doi: 10.1029/WR014i004p00601

Cook, B. I., Ault, T. R., and Smerdon, J. E. (2015). Unprecedented 21st century drought risk in the American southwest and central plains. *Sci. Adv*. 1, e1400082. doi: 10.1126/sciadv.1400082

Cook, B. I., Mankin, J. S., and Anchukaitis, K. J. (2018). Climate change and drought: from past to future. *Curr. Clim. Change Rep*. 4, 164–179. doi: 10.1007/s40641-018-0093-2

Costa, F. R. C., Schietti, J., Stark, S. C. and Smith, M. N. (2022). The other side of tropical forest drought: do shallow water table regions of Amazonia act as large-scale hydrological refugia from drought?. *New Phytol*. doi: 10.1111/nph.17914 [Epub ahead of print].

Crouchet, S. E., Jensen, J., Schwartz, B. F., and Schwinning, S. (2019). Tree mortality after a hot drought: distinguishing density-dependent and-independent drivers and why it matters. *Front. For. Glob. Change* 2, 21. doi: 10.3389/ffgc.2019.00021

Cutler, A., Cutler, D. R., and Stevens, J. R. (2012). "Random forests," in *Ensemble Machine Learning* (Boston, MA: Springer), 157–175. doi: 10.1007/978-1-4419-9326-7_5

Dai, A., Trenberth, K. E., and Qian, T. (2004). A global dataset of palmer drought severity index for 1870-2002: relationship with soil moisture and effects of surface warming. *J. Hydrometeorol*. 5, 1117–1130. doi: 10.1175/JHM-386.1

D'Amato, A. W., Bradford, J. B., Fraver, S., and Palik, B. J. (2013). Effects of thinning on drought vulnerability and climate response in north temperate forest ecosystems. *Ecol. Appl*. 23, 1735–1742. doi: 10.1890/13-0677.1

Déqué, M. (2007). Frequency of precipitation and temperature extremes over France in an anthropogenic scenario: model results and statistical correction according to observed values. *Glob. Planet. Change* 57, 16–26. doi: 10.1016/j.gloplacha.2006.11.030

D'Orangeville, L., Houle, D., Duchesne, L., and Côté, B. (2016). Can the Canadian drought code predict low soil moisture anomalies in the mineral soil? An analysis of 15 years of soil moisture data from three forest ecosystems in eastern Canada. *Ecohydrology* 9, 238–247. doi: 10.1002/eco.1627

D'Orangeville, L., Maxwell, J., Kneeshaw, D., Pederson, N., Duchesne, L., Logan, T., et al. (2018). Drought timing and local climate determine the sensitivity of eastern temperate forests to drought. *Glob. Change Biol*. 24, 2339–2351. doi: 10.1111/gcb.14096

Eckes-Shephard, A. H., Tiavlovsky, E., Chen, Y., Fonti, P., and Friend, A. D. (2021). Direct response of tree growth to soil water and its implications for terrestrial carbon cycle modelling. *Glob. Change Biol*. 27, 121–135. doi: 10.1111/gcb.15397

Ficklin, D. L., and Novick, K. A. (2017). Historic and projected changes in vapor pressure deficit suggest a continental-scale drying of the United States atmosphere. *J. Geophys. Res*. 122, 2061–2079. doi: 10.1002/2016JD025855

Field, J. P., Breshears, D. D., Bradford, J. B., Law, D. J., Feng, X., and Allen, C. D. (2020). Forest management under megadrought: urgent needs at finer scale and higher intensity. *Front. For. Glob. Change* 3, 140. doi: 10.3389/ffgc.2020.502669

Fisher, R. A., and Koven, C. D. (2020). Perspectives on the future of land surface models and the challenges of representing complex terrestrial systems. *J. Adv. Model. Earth Syst*. 12, e2018MS001453. doi: 10.1029/2018MS001453

Fu, Z., Ciais, P., Makowski, D., Bastos, A., Stoy, P. C., Ibrom, A., et al. (2021). Uncovering the critical soil moisture thresholds of plant water stress for European ecosystems. *Glob. Change Biol*. 28, 2111–2123. doi: 10.1111/gcb.16050

Gazol, A., Camarero, J. J., Vicente-Serrano, S. M., Sánchez-Salguero, R., Gutiérrez, E., de Luis, M., et al. (2018). Forest resilience to drought varies across biomes. *Glob. Change Biol*. 24, 2143–2158. doi: 10.1111/gcb.14082

Gerten, D., Luo, Y., Le Maire, G., Parton, W. J., Keough, C., Weng, E., et al. (2008). Modelled effects of precipitation on ecosystem carbon and water dynamics in different climatic zones. *Glob. Change Biol*. 14, 2365–2379. doi: 10.1111/j.1365-2486.2008.01651.x

Grant, G. E., Tague, C. L., and Allen, C. D. (2013). Watering the forest for the trees: an emerging priority for managing water in forest landscapes. *Front. Ecol. Environ*. 11, 314–321. doi: 10.1890/120209

Grondin, P., Gauthier, S., Poirier, V., Tardif, P., Boucher, Y., and Bergeron, Y. (2018). Have some landscapes in the eastern Canadian boreal forest moved beyond their natural range of variability? *For. Ecosyst*. 5, 1–17. doi: 10.1186/s40663-018-0148-9

Gudmundsson, L., and Seneviratne, S. I. (2016). Anthropogenic climate change affects meteorological drought risk in Europe. *Environ. Res. Lett*. 11, 044005. doi: 10.1088/1748-9326/11/4/044005

Haghnegahdar, A., Tolson, B. A., Craig, J. R., and Paya, K. T. (2015). Assessing the performance of a semi-distributed hydrological model under various watershed discretization schemes. *Hydrol. Process*. 29, 4018–4031. doi: 10.1002/hyp.10550

He, L., Ivanov, V. Y., Bohrer, G., Maurer, K. D., Vogel, C. S., and Moghaddam, M. (2014). Effects of fine-scale soil moisture and canopy heterogeneity on energy and water fluxes in a northern temperate mixed forest. *Agric. For. Meteorol*. 184, 243–256. doi: 10.1016/j.agrformet.2013.10.006

Hember, R. A., Kurz, W. A., and Coops, N. C. (2017). Relationships between individual-tree mortality and water-balance variables indicate positive trends in water stress-induced tree mortality across North America. *Glob. Change Biol*. 23, 1691–1710. doi: 10.1111/gcb.13428

Hersbach, H., Bell, B., Berrisford, P., Hirahara, S., Horányi, A., Mu noz-Sabater, J., et al. (2020). The era5 global reanalysis. *Q. J. R. Meteorol. Soc*. 146, 1999–2049. doi: 10.1002/qj.3803

Hoffmann, W. A., Marchin, R. M., Abit, P., and Lau, O. L. (2011). Hydraulic failure and tree dieback are associated with high wood density in a temperate forest under extreme drought. *Glob. Change Biol*. 17, 2731–2742. doi: 10.1111/j.1365-2486.2011.02401.x

Houle, D., Bouffard, A., Duchesne, L., Logan, T., and Harvey, R. (2012). Projections of future soil temperature and water content for three southern Quebec forested sites. *J. Clim*. 25, 7690–7701. doi: 10.1175/JCLI-D-11-00440.1

Houle, D., Harvey, R., Logan, T., and Duchesne, L. (2014). *Développement D'indicateurs Hydro-Climatiques: Projection des Changements de Température et D'humidité des Sols Forestiers et de Leurs Impacts Potentiels sur la Fertilité des Sols*. Report Impact et adaptation, Programme ICAR-Quebec, Volet Foresterie.

Jackson, R. B., Canadell, J., Ehleringer, J. R., Mooney, H., Sala, O., and Schulze, E.-D. (1996). A global analysis of root distributions for terrestrial biomes. *Oecologia* 108, 389–411. doi: 10.1007/BF00333714

Maheu, A., Cholet, C., Montoya, R. C, and Duchesne, L. (2021). Is the annual maximum leaf area index an important driver of water fluxes simulated by a land surface model in temperate forests?. *Canad. J. Forest. Res*. 51, 595–603. doi: 10.1139/cjfr-2020-0126

Marchin, R. M., Ossola, A., Leishman, M. R., and Ellsworth, D. S. (2020). A simple method for simulating drought effects on plants. *Front. Plant Sci*. 2019, 1715. doi: 10.3389/fpls.2019.01715

Martynov, A., Laprise, R., Sushama, L., Winger, K., Šeparović, L., and Dugas, B. (2013). Reanalysis-driven climate simulation over cordex North America domain using the Canadian regional climate model, version 5: model performance evaluation. *Clim. Dyn*. 41, 2973–3005. doi: 10.1007/s00382-013-1778-9

May, W. (2008). Potential future changes in the characteristics of daily precipitation in Europe simulated by the Hirham regional climate model. *Clim. Dyn*. 30, 581–603. doi: 10.1007/s00382-007-0309-y

McKenney, D. W., Hutchinson, M. F., Papadopol, P., Lawrence, K., Pedlar, J., Campbell, K., et al. (2011). Customized spatial climate models for North America. *Bull. Am. Meteorol. Soc*. 92, 1611–1622. doi: 10.1175/2011BAMS3132.1

McLaughlin, B. C., Ackerly, D. D., Klos, P. Z., Natali, J., Dawson, T. E., and Thompson, S. E. (2017). Hydrologic refugia, plants, and climate change. *Glob. Change Biol*. 23, 2941–2961. doi: 10.1111/gcb.13629

Mekonnen, M., Soulis, R., Fortin, V., Davidson, B., Marin, S., and Wilson, R. (2012). *WATDRN: Enhanced Hydrology for Class*. Technical paper.

MELCC (2018). *Base de Données des Lacs et Cours d'eau (LCE) du Territoire Québecois*. MELCC. Available online at: https://www.donneesquebec.ca/recherche/dataset/base-de-donnees-des-lacs-et-cours-d-eau-lce# (accessed February 1, 2019).

MFFP (2015). *Produits dérivés du LiDAR généré Dans le Cadre du Projet D'acquisition de Données par le Capteur LiDAR á l'échelle Provincial*. MFFP.

Available online at: https://www.donneesquebec.ca/recherche/fr/dataset/produits-derivesde-base-du-lidar

MFFP (2018). *Cartographie du 5e Inventaire Écoforestier du Québec Méridional - Méthodes et Données associées*. Ministére des Forêts, de la Faune et des Parcs, Secteur des forêts, Direction des Inventaires Forestiers, 111.

Millar, C. I., and Stephenson, N. L. (2015). Temperate forest health in an era of emerging megadisturbance. *Science* 349, 823–826. doi: 10.1126/science.aaa9933

Myneni, R., Knyazikhin, Y., and Park, T. (2015). *Mod15a2h Modis/Terra Leaf Area Index/Fpar 8-day l4 Global 500 m Sin Grid V006*. NASA EOSDIS Land Processes DAAC.

Pan, Y., Birdsey, R. A., Fang, J., Houghton, R., Kauppi, P. E., Kurz, W. A., et al. (2011). A large and persistent carbon sink in the world's forests. *Science* 333, 988–993. doi: 10.1126/science.1201609

Pettijohn, J. C., Salvucci, G. D., Phillips, N. G., and Daley, M. J. (2009). Mechanisms of moisture stress in a mid-latitude temperate forest: implications for feedforward and feedback controls from an irrigation experiment. *Ecol. Model.* 220, 968–978. doi: 10.1016/j.ecolmodel.2008.12.020

Pietroniro, A., Fortin, V., Kouwen, N., Neal, C., Turcotte, R., Davison, B., et al. (2007). Development of the mesh modelling system for hydrological ensemble forecasting of the Laurentian great lakes at the regional scale. *Hydrol. Earth Syst. Sci. Discuss*. 11, 1279–1294. doi: 10.5194/hess-11-1279-2007

Prudhomme, C., Giuntoli, I., Robinson, E. L., Clark, D. B., Arnell, N. W., Dankers, R., et al. (2014). Hydrological droughts in the 21st century, hotspots and uncertainties from a global multimodel ensemble experiment. *Proc. Natl. Acad. Sci. U.S.A*. 111, 3262–3267. doi: 10.1073/pnas.1222473110

Ranney, T., Whitlow, T., and Bassuk, N. (1990). Response of five temperate deciduous tree species to water stress. *Tree Physiol.* 6, 439–448. doi: 10.1093/treephys/6.4.439

Royer-Tardif, S., Bauhus, J., Doyon, F., Nolet, P., Thiffault, N., and Aubin, I. (2021). Revisiting the functional zoning concept under climate change to expand the portfolio of adaptation options. *Forests* 12, 273. doi: 10.3390/f12030273

Ruffault, J., Martin-StPaul, N. K., Rambal, S., and Mouillot, F. (2013). Differential regional responses in drought length, intensity and timing to recent climate changes in a Mediterranean forested ecosystem. *Clim. Change* 117, 103–117. doi: 10.1007/s10584-012-0559-5

Samaniego, L., Thober, S., Kumar, R., Wanders, N., Rakovec, O., Pan, M., et al. (2018). Anthropogenic warming exacerbates European soil moisture droughts. *Nat. Clim. Change* 8, 421–426. doi: 10.1038/s41558-018-0138-5

Sanborn, P., Lamontagne, L., and Hendershot, W. (2011). Podzolic soils of Canada: genesis, distribution, and classification. *Can. J. Soil Sci*. 91, 843–880. doi: 10.4141/cjss10024

Saucier, J.-P., Grondin, A., Robitaille, J., Gosselin, C., Morneau, P., Richard, P., et al. (2009). *Ecologie Forestiére, Dans Ordre Des Ingenieurs Forestiers Du Quebec, 2nd Edn*. Québec, QC: Manuel de Foresterie.

Schindlbacher, A., Wunderlich, S., Borken, W., Kitzler, B., Zechmeister-Boltenstern, S., and Jandl, R. (2012). Soil respiration under climate change: prolonged summer drought offsets soil warming effects. *Glob. Change Biol.* 18, 2270–2279. doi: 10.1111/j.1365-2486.2012.02696.x

Schwantes, A. M., Parolari, A. J., Swenson, J. J., Johnson, D. M., Domec, J.-C., Jackson, R. B., et al. (2018). Accounting for landscape heterogeneity improves spatial predictions of tree vulnerability to drought. *New Phytol.* 220, 132–146. doi: 10.1111/nph.15274

Šeparović, L., Alexandru, A., Laprise, R., Martynov, A., Sushama, L., Winger, K., et al. (2013). Present climate and climate change over North America as simulated by the fifth-generation Canadian regional climate model. *Clim. Dyn.* 41, 3167–3201. doi: 10.1007/s00382-013-1737-5

Soulis, E. D., Snelgrove, K. R., Kouwen, N., Seglenieks, F., and Verseghy, D. L. (2000). Towards closing the vertical water balance in Canadian atmospheric models: coupling of the land surface scheme class with the distributed hydrological model Watflood. *Atmos. Ocean* 38, 251–269. doi: 10.1080/07055900.2000.9649648

Sperry, J., Hacke, U., Oren, R., and Comstock, J. (2002). Water deficits and hydraulic limits to leaf water supply. *Plant Cell Environ.* 25, 251–263. doi: 10.1046/j.0016-8025.2001.00799.x

Stevens, D., Miranda, P., Orth, R., Boussetta, S., Balsamo, G., and Dutra, E. (2020). Sensitivity of surface fluxes in the ECMWF land surface model to the remotely sensed leaf area index and root distribution: Evaluation with tower flux data. *Atmosphere* 11, 1362. doi: 10.3390/atmos11121362

Stocker, T. (2014). *Climate Change 2013: The Physical Science Basis: Working Group I Contribution to the Fifth Assessment Report of the Intergovernmental Panel on Climate Change*. Cambridge University Press.

Sushama, L., Khaliq, N., and Laprise, R. (2010). Dry spell characteristics over Canada in a changing climate as simulated by the Canadian RCM. *Glob. Planet. Change* 74, 1–14. doi: 10.1016/j.gloplacha.2010.07.004

Sylvain, J.-D., Anctil, F., and Thiffault, É. (2021). Using bias correction and ensemble modelling for predictive mapping and related uncertainty: a case study in digital soil mapping. *Geoderma* 403, 115153. doi: 10.1016/j.geoderma.2021.115153

Tarek, M., Brissette, F. P., and Arsenault, R. (2020). Evaluation of the ERA5 reanalysis as a potential reference dataset for hydrological modelling over North America. *Hydrol. Earth Syst. Sci*. 24, 2527–2544. doi: 10.5194/hess-24-2527-2020

Tauc, F., Houle, D., Dupuch, A., Doyon, F., and Maheu, A. (2020). Microtopographic refugia against drought in temperate forests: lower water availability but more extensive fine root system in mounds than in pits. *For. Ecol. Manage.* 476, 118439. doi: 10.1016/j.foreco.2020.118439

Trenberth, K. E., Dai, A., Van Der Schrier, G., Jones, P. D., Barichivich, J., Briffa, K. R., and Sheffield, J. (2014). Global warming and changes in drought. *Nat. Clim. Change* 4, 17–22. doi: 10.1038/nclimate2067

Vanderborght, J., Couvreur, V., Meunier, F., Schnepf, A., Vereecken, H., Bouda, M., et al. (2021). From hydraulic root architecture models to macroscopic representations of root hydraulics in soil water flow and land surface models. *Hydrol. Earth Syst. Sci.* 25, 4835–4860. doi: 10.5194/hess-25-4835-2021

Verseghy, D., McFarlane, N., and Lazare, M. (1993). Class-a Canadian land surface scheme for GCMS, II. Vegetation model and coupled runs. *Int. J. Climatol.* 13, 347–370. doi: 10.1002/joc.3370130402

Verseghy, D. L. (1991). Class-a Canadian land surface scheme for GCMS. I. Soil model. *Int. J. Climatol.* 11, 111–133. doi: 10.1002/joc.3370110202

Verseghy, D. L. (2000). The Canadian land surface scheme (class): its history and future. *Atmosphere* 38, 1–13. doi: 10.1080/07055900.2000.9649637

Verseghy, D. L. (2012). *Class-the Canadian Land Surface Scheme (Version 3.6)*. Environment Canada Science and Technology Branch Technical Report.

Williams, A. P., Cook, E. R., Smerdon, J. E., Cook, B. I., Abatzoglou, J. T., Bolles, K., Baek, S. H., Badger, A. M., and Livneh, B. (2020). Large contribution from anthropogenic warming to an emerging North American megadrought. *Science* 368, 314–318. doi: 10.1126/science.aaz9600

Yu, G.-R., Zhuang, J., Nakayama, K., and Jin, Y. (2007). Root water uptake and profile soil water as affected by vertical root distribution. *Plant Ecol.* 189, 15–30. doi: 10.1007/s11258-006-9163-y

Yuan, W., Zheng, Y., Piao, S., Ciais, P., Lombardozzi, D., Wang, Y., Ryu, Y., Chen, G., Dong, W., Hu, Z., et al. (2019). Increased atmospheric vapor pressure deficit reduces global vegetation growth. *Sci. Adv.* 5, eaax1396. doi: 10.1126/sciadv.aax1396

Zhao, T. and Dai, A. (2015). The magnitude and causes of global drought changes in the twenty-first century under a low-moderate emissions scenario. *J. Clim.* 28, 4490–4512. doi: 10.1175/JCLI-D-14-00363.1

Conflict of Interest: The authors declare that the research was conducted in the absence of any commercial or financial relationships that could be construed as a potential conflict of interest.

Publisher's Note: All claims expressed in this article are solely those of the authors and do not necessarily represent those of their affiliated organizations, or those of the publisher, the editors and the reviewers. Any product that may be evaluated in this article, or claim that may be made by its manufacturer, is not guaranteed or endorsed by the publisher.